

Magnetic response of carbon nanotubes from *ab initio* calculations

Miguel A. L. Marques, Mayeul d’Avezac, and Francesco Mauri
*Institut de Minéralogie et de Physique des Milieux Condensés,
Université Paris VI, 140 rue de Lourmel 75015 Paris, France*
(Dated: May 1, 2019)

We present *ab initio* calculations of the magnetic susceptibility and of the ^{13}C chemical shift for carbon nanotubes, both isolated and in bundles. These calculations are performed using the recently proposed gauge-including projector augmented-wave approach for the calculation of magnetic response in periodic insulating systems. We have focused on the semiconducting zigzag nanotubes with diameters ranging from 0.6 to 1.6 nm. Both the susceptibility and the isotropic shift exhibit a dependence with the diameter (D) and the chirality of the tube (although this dependence is stronger for the susceptibility). The isotropic shift behaves asymptotically as $\alpha/D + 116.0$, where α is a different constant for each family of nanotubes. For a tube diameter of around 1.2 nm, a value normally found in experimental samples, our results are in excellent agreement with experiments. Moreover, we calculated the chemical shift of a double-wall tube. We found a diamagnetic shift of the isotropic lines corresponding to the atoms of the inner tube due to the effect of the outer tube. This shift is in good agreement with recent experiments, and can be easily explained by demagnetizing currents circulating the outer tube.

PACS numbers: 61.46.+w, 76.60.Cq, 71.15.Mb

I. INTRODUCTION

Carbon nanotubes are indubitably among of the most interesting materials discovered in the past years^{1,2}. From a theoretical point of view, their quasi one-dimensional character imposes quite exotic electronic properties. In fact, some time ago it was proposed that carbon nanotubes might be good candidates for the elusive Luttinger liquids³. From a more practical point of view, carbon nanotubes turned out to be extraordinary materials, as they possess remarkable mechanical and electronic properties. This makes them probable building blocks for future high-stiffness materials and molecular nanodevices⁴. The electronic properties of single-wall carbon nanotubes (SWCNT) can be tuned by varying the two integers (n, m) which determine the chirality of the tube. For instance nanotubes are either metallic (for $n = m$) or semiconducting. In the latter case, the band gap can range from more than 1 eV [e.g., 1.31 eV for the (4,3) tube⁵] to nearly zero [e.g., for tubes with $\ell = 0$, where $\ell = \text{mod}(n - m, 3)$ labels the “family” to which the SWCNT belongs].

Among various experimental techniques that can be used to study and characterize materials, nuclear magnetic resonance (NMR) stands out as being particularly suited to study local electronic structures⁶. NMR is widely used in structural chemistry and in material science. It measures the local magnetic fields on the nuclei generated by the response of the electrons to an external uniform magnetic field. In nonmagnetic insulators this response (the chemical shift) is determined by the orbital motion of the electrons, and provides information about the local atomic environment (coordination and geometry) around each nucleus.

In spite of the usefulness of the technique, only a few groups have up to now used NMR to study carbon nan-

otubes. The reason is that these experiments are quite difficult to perform, due to the presence of magnetic impurities (like Rh, Pt, Ni, etc.) in the samples. These impurities, which are added as a catalyst during the production of the nanotubes, lead to very broad magic-spinning angle (MAS) spectra, with widths of about 30–50 ppm^{7,8,9}. However, we expect this situation to change soon, due to new production techniques that use water¹⁰ or alcohol¹¹ to enhance the activity and the lifetime of the catalysts. In this way, it is possible to produce samples with a SWCNT/catalyst weight ratio 100 times higher than previous techniques¹⁰, which will clearly allow the measurement of NMR spectra to unprecedented accuracy. Another possible approach involves the removal of the ferromagnetic impurities in solution. This very promising path has been used recently to study the NMR response of functionalized (soluble) nanotubes¹².

In this paper, we perform a *ab initio* study of the magnetic response properties of *infinite* carbon nanotubes. In particular, we provide benchmark calculations of the magnetic susceptibility and NMR ^{13}C chemical shift of semiconducting SWCNT, both isolated and in bundles. Furthermore, we present results for double-wall tubes.

II. COMPUTATIONAL DETAILS

We use the recently proposed gauge-including projector augmented-wave (GIPAW) approach for the calculation of NMR response in periodic systems¹³. This approach is based on a linear response formulation of density functional theory (DFT), as implemented in the plane-wave pseudo-potential code PARATEC¹⁴. Contributions to the NMR spectra from the core regions are taken into account using the projector augmented-wave (PAW) electronic structure method¹⁵. We would like to

remark that the current implementation of the GIPAW method only allows the study of semiconducting systems. The extension to metals is currently on the way, and first results are expected shortly.

We restrict our study to $(n, 0)$ (zigzag) nanotubes, belonging to the two families characterized by $\ell = 1$ ($n = 10, 13, 16, 19$) and $\ell = 2$ ($n = 8, 11, 14, 17, 20$). For each of these families, the band gap decreases as $1/D$, where D is the diameter of the tube. (Note that zigzag tubes have a relatively small number of atoms in the unit cell, which eases the computational burden.) In all calculations, wave-functions were expanded in plane-waves with a cutoff of 40 Ry, and we used the PBE generalized gradient approximation to the exchange and correlation functional of DFT. For carbon, we used a norm conserving Troullier-Martins¹⁶ pseudo-potential with a core radius of 1.75 a.u. The GIPAW reconstruction included two projectors per angular momentum for both s and p electrons.

The “isolated” tubes were rolled from a graphene sheet with $C - C = 1.43 \text{ \AA}$ and were set in a tetragonal superlattice, with a minimum separation of 5.5 \AA between neighboring tubes. For the smaller tubes a sampling of 20 k-points in the periodic dimension proved sufficient to converge our results to better than 0.25 ppm, while larger tubes required 40 k-points at most. We modeled bundles by arranging nanotubes on a hexagonal lattice, with an inter-tube spacing of 3.3 \AA . In the plane perpendicular to the tube axis, we used a 4×4 sampling of the irreducible Brillouin zone. Overall, we believe that our numerical procedure yields magnetic susceptibilities to a couple of percent and isotropic shifts with a precision better than 1 ppm.

When calculating the chemical shift tensor, special care has to be taken with its macroscopic component $\sigma(\mathbf{G} = 0)$. This is not a bulk quantity, and its value depends on the shape of the macroscopic sample. For example, for a spherical or cylindrical sample, and for a susceptibility tensor diagonal in the Cartesian axis, this quantity can be related to the volumetric macroscopic susceptibility χ_V through the relation (in cgs units)

$$\sigma(\mathbf{0}) = -4\pi\alpha\chi_V, \quad (1)$$

where α is a diagonal matrix with values $\alpha_{ii} = 2/3$ for a sphere and $\alpha_{xx} = \alpha_{yy} = 1/2$ and $\alpha_{zz} = 1$ for a cylinder (in this latter case z denotes the direction of the axis of the cylinder). In the case of a bundle of nanotubes, we believe that the most correct choice is the cylinder. For the isolated tubes the volumetric macroscopic susceptibility decays as $1/A^2$, where A is the distance between the centers of two adjacent tubes. We are therefore free to choose the matrix α in order to speed up the convergence of the chemical shift with A . We found empirically that the choice $\alpha_{xx} = \alpha_{yy} = 1/2$ and $\alpha_{zz} = 2/3$ provided a faster convergence rate than either the sphere or the cylinder.

Experimental results for the chemical shift are usually given relatively to the isotropic shift of tetramethylsi-

lane (TMS). The reference TMS shielding tensor σ_{TMS} is usually calculated within the same numerical framework used for the systems under study. This is, e.g., the method used in Ref. 17. In this work, we follow a slightly different approach. Within our GIPAW method we calculate the ^{13}C shielding tensor of benzene, and use the formula

$$\delta_{\text{tube}}^{\text{TMS}} = -(\sigma_{\text{tube}} - \sigma_{\text{benzene}}^{\text{iso}}) + \delta_{\text{benzene}}^{\text{TMS}}, \quad (2)$$

where σ_{tube} is the *calculated* shielding tensor of the tube and $\sigma_{\text{benzene}}^{\text{iso}}$ is the average value of the diagonal of the *calculated* shielding tensor of benzene. Finally, $\delta_{\text{benzene}}^{\text{TMS}}$ is the *experimental* isotropic chemical shift in the gas-phase of benzene relative to TMS. As the magnetic response of the tubes is very similar to the response of benzene, we expect in this way to minimize the systematic errors in our calculations. The experimental $\delta_{\text{benzene}}^{\text{TMS}}$ was taken to be 126.9 ppm¹⁸, while $\sigma_{\text{benzene}}^{\text{iso}}$ calculated at the equilibrium geometry was 40.0 ppm.

III. MAGNETIC SUSCEPTIBILITY

The magnetic susceptibility (χ) of SWCNTs has already been the subject of two theoretical studies: (i) Ajiki and Ando¹⁹ using the $\mathbf{k}\cdot\mathbf{p}$ perturbation method, and (ii) Lu²⁰ using a tight-binding approach within the London approximation. It was found that χ increases linearly with the nanotube diameter. Furthermore, for an applied magnetic field parallel to the tube axis, the response χ_{\parallel} was paramagnetic for tubes with $\ell = 0$, while for tubes with $\ell = 1$ or 2 the response was diamagnetic. In contrast, for a field perpendicular to the axis of the tube, all nanotubes were diamagnetic. Finally, it was found that the response of the tubes with $\ell = 1$ and $\ell = 2$ was almost identical.

The experimental situation is somehow more complicated, as the experimental samples normally contain a mixture of tubes of different chiralities, including both metallic and semiconducting tubes. However, a recent experiment²¹ estimated the magnitude of the magnetic susceptibility anisotropy $\chi_{\parallel} - \chi_{\perp}$ to be $\sim 14 \times 10^{-6}$ cgs/mol for 1 nm diameter semiconducting tubes, similar to the predicted values of 19×10^{-6} cgs/mol (Ref. 19) and 15×10^{-6} cgs/mol (Ref. 20).

In Fig. 1 we plot our *ab initio* results for the magnetic susceptibility tensor of the isolated tubes. In contrast with Refs. 19 and 20 we can clearly distinguish the two families of semiconducting zigzag tubes. For the family with $\ell = 2$, χ_{\parallel}/D is very weakly dependent on n , while for the other family ($\ell = 1$) the absolute value of χ_{\parallel}/D decreases slowly with the diameter of the tube. For χ_{\perp} the situation is reversed: This quantity is almost independent of n for $\ell = 1$, and its absolute value decreases monotonically for $\ell = 2$. Note that, if we extrapolate our results to $D \rightarrow \infty$, we find values quite consistent with Ref. 20.

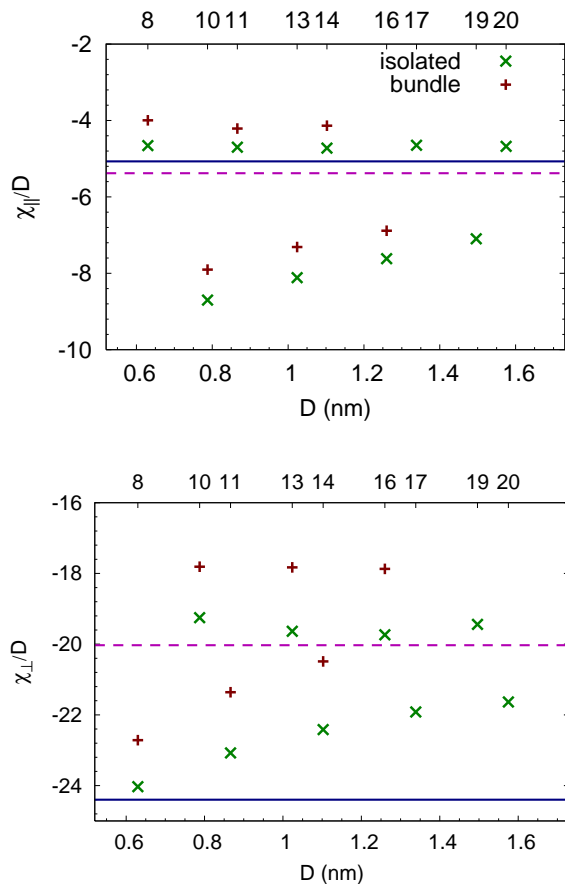


FIG. 1: (Color online) Magnetic susceptibility of zigzag semi-conducting nanotubes, both isolated and in bundles, *vs* diameter (D) of the tube. The blue (solid) lines correspond to the results of Ref. 19 ($\chi_{\parallel}/D = -5.1$ and $\chi_{\perp}/D = -24.4$) and the violet (dashed) lines correspond to Ref. 20 ($\chi_{\parallel}/D = -5.4$ and $\chi_{\perp}/D = -20.0$). The upper axis labels the chirality ($n, 0$) of the tube. All results are in 10^{-6} cgs/(nm mol).

For a 1 nm diameter tube, we obtain for the magnetic susceptibility anisotropy ($\chi_{\parallel} - \chi_{\perp}$) values between ~ 12 and $\sim 18 \times 10^{-6}$ cgs/mol depending on the chirality of the tube. This result is in quite good agreement with the value $\chi_{\parallel} - \chi_{\perp} = 14 \times 10^{-6}$ cgs/mol measured in Ref. 21.

Regarding the bundles, we can see from Fig. 1 that their magnetic susceptibility is very similar to the one of isolated tubes. The main difference is a (fairly rigid) decrease of χ_{\parallel}/D by around 0.5×10^{-6} cgs/(nm mol) and of χ_{\perp}/D by around 1×10^{-6} cgs/(nm mol).

IV. CHEMICAL SHIFT

Only a few groups have studied carbon nanotubes *via* NMR, whether experimentally or theoretically. Experimental ^{13}C MAS spectra of pristine tubes yield isotropic shifts²⁷ δ_{iso} of 126 ppm^{7,8}, 124 ppm²², and 116 ppm⁹. The full width at half maximum (FWHM) of the isotropic

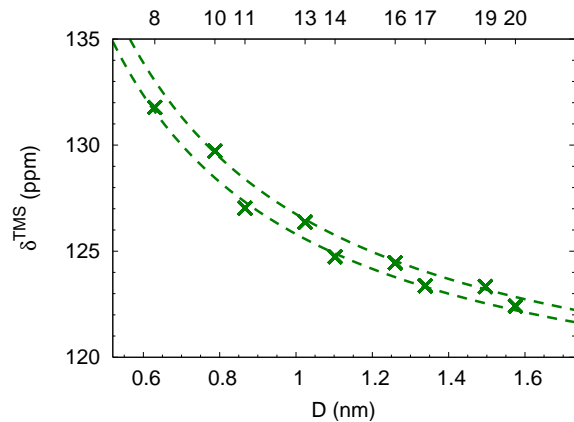


FIG. 2: (Color online) Isotropic chemical shifts for the isolated zigzag nanotubes, versus diameter (D) of the tube. The lines are the fits to the numerical results given by Eq. (3).

peak is fairly large, being around 50 ppm^{7,8} or 30 ppm⁹. This width was interpreted as a distribution of isotropic lines, resulting in part from the presence of both semi-conducting and metallic tubes in the sample. The static spectra are quite broad, spawning more than 200 ppm. It was also noted that the presence of residual Ni and Co magnetic particles can contribute to the further broadening of the spectra.

The principal values of the chemical shift tensor can be obtained from the NMR spectra through a fitting procedure. In this way, Ref. 22 found $\delta_{11}^{\text{TMS}} = 195$ ppm, $\delta_{22}^{\text{TMS}} = 160$ ppm, and $\delta_{33}^{\text{TMS}} = 17$ ppm (which leads to $\Delta\delta_{\text{anis}} = -160.5$ ppm and $\eta_{\text{C}} = 0.33$), while in Ref. 8 it was obtained $\delta_{11}^{\text{TMS}} = 240$ ppm, $\delta_{22}^{\text{TMS}} = 171$ ppm, and $\delta_{33}^{\text{TMS}} = -36$ ppm ($\Delta\delta_{\text{anis}} = -241.5$ ppm and $\eta_{\text{C}} = 0.43$). The large difference between the two experiments (see Fig. 4) can be understood from the difficulty of obtaining good samples.

On the theoretical side, the first attempt at describing the NMR response of carbon nanotubes²³ was performed within a tight-binding scheme and using the London approximation (i.e., retaining only the London ring-current contribution to the chemical shift and neglecting the Pople correction²⁴). To justify this approximation it was argued that the Pople contribution gave rise to a global shift, independent of chirality, that could not be used to distinguish between different tubes. Within this framework, it was estimated that the difference in the isotropic chemical shift between metallic and semi-conducting tubes amounted to 12 ppm. (Absolute shifts were not given due to the neglect of the Pople correction.) Furthermore, it was found that the NMR of both metallic and semiconducting is mostly insensitive to diameter and chirality.

More recently the ^{13}C chemical shift of finite-size (9,0) single wall carbon nanotubes was investigated¹⁷. The tube fragments studied were capped by either C_{30} or hydrogen. For the longest fragment it was found $\delta_{\text{iso}}^{\text{TMS}} \approx$

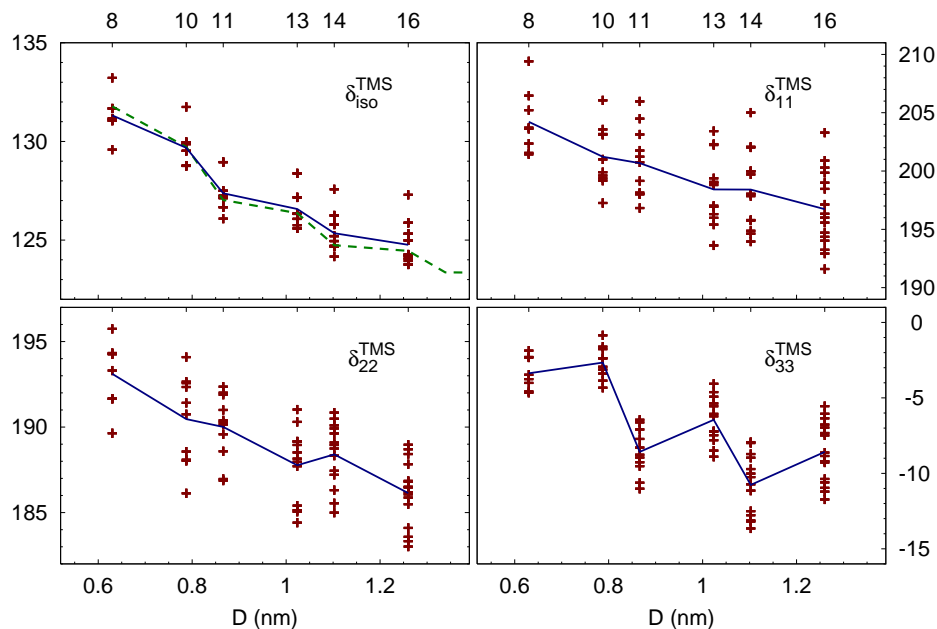


FIG. 3: (Color online) Chemical shifts relative to TMS for the zigzag nanotubes in bundles versus radius of the tube. The blue (solid) lines connect the average values for each tube. The green (dashed) line is the results for the isolated tubes presented before.

133 ppm for carbon atoms at the center of tube, in reasonably good agreement with experimental data. For the C_{30} -capped tubes, apparently the best models for the infinite systems, the shifts in the middle of the fragment were invariably smaller than those at the end (where they reached $\delta_{\text{iso}}^{\text{TMS}} \approx 155$ ppm).

A. Isotropic shift

Our results for the isolated tubes are presented in Fig. 2. The two families can be clearly identified: The family with $\ell = 1$ has a slightly larger chemical shift than the family with $\ell = 2$. The results can be fitted by the relation

$$\delta_{\text{iso}}^{\text{TMS}} = \begin{cases} 10.70/D + 116.0 & \text{if } \ell = 1 \\ 9.83/D + 116.0 & \text{if } \ell = 2 \end{cases}, \quad (3)$$

where D is the diameter of the nanotube in nanometers, and $\delta_{\text{iso}}^{\text{TMS}}$ is the isotropic chemical shift relative to TMS in ppm. According to this formula, in the limit of infinite radius the isotropic chemical shift tends to 116.0 ppm. This value compares reasonably well with the estimate of 128 ppm for $\delta_{\text{graphene}}^{\text{TMS}}$ of a perfect graphene layer (with zero density of states at the Fermi level)^{8,25}. For a nanotube with a diameter of 1.2 nm, like the ones common in experimental samples, we obtain a $\delta_{\text{iso}} \approx 125$ ppm, in excellent agreement with experiment^{7,8,9,22}. Note that, as already indicated in Refs. 7 and 8, the NMR chemical shift depends very weakly on the diameter and on the chirality of the semiconducting nanotubes: the isotropic

shifts of the zigzag tubes studied in this work lie between 122 ppm for the smallest tube [the (8, 0)] to 132 ppm for the (20, 0) tube.

The isotropic shifts of the bundles are represented by red crosses in Fig. 3. Since the hexagonal lattice breaks the chiral symmetry of the tubes, the carbon atoms around the circumference of the tube are no longer equivalent, resulting in a slight spread of δ^{TMS} in the unit cell. For the nanotubes studied here, this spread of the isotropic shift was quite small (around 3 ppm), and fairly independent of the radius of the tube. It can also be seen that the average shift in a bundle is nearly equal to the isotropic value of the isolated tube⁸.

We are now in condition to discuss the large width MAS spectra, that amounts to 30–50 ppm. Several effects can contribute to this width:

(i) Experimental samples are composed of nanotubes of different diameters and chiralities. Assuming that the spread of diameters is around 0.5 nm, and the distribution is centered around 1.2 nm, from Fig 2 we obtain a spread of around 4 ppm. Furthermore, the difference in chemical shift between semiconducting and metallic tubes was estimate to be 12 ppm⁸.

(ii) As experiments are usually performed with samples of SWCNTs arranged in bundles, we have to take into account the spread of isotropic chemical shifts due to the breaking of chiral symmetry. As we saw from Fig. 3 this amounts to around 3 ppm for zigzag tubes.

(iii) As mentioned before, in order to obtain the macroscopic component of the chemical shift tensor, we assumed that the bundle was of cylindrical shape. However,

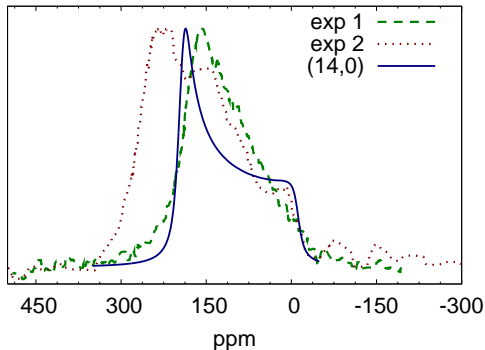


FIG. 4: (Color online) Experimental versus simulated static spectra for the carbon nanotubes. The curve labeled 'exp 1' was taken from Ref. 22, while 'exp 2' was taken from Ref. 8. The theoretical curve corresponds to the static spectrum of a bundle of (14,0) nanotubes, convoluted with a Lorentzian of 30 ppm FWHM.

in a real sample, the bundle can assume shapes quite different from a perfect cylinder. To address this issue, we performed calculations assuming a spherical shape for the bundle. For the (14,0) tube, a typical nanotube of 1.1 nm diameter, the isotropic shift calculated for the cylinder was 125.3 ppm, while the sphere gave 122.4 ppm. Note that, even if the difference, 3 ppm, is much smaller than the experimental width of the MAS spectrum, it has nevertheless the same magnitude as the difference between nanotubes of similar diameter.

(iv) Finite-size SWCNTs can be either open, or capped by fullerene-like structures. It was found in Ref. 17 that the carbon atoms close to the ends of these (finite) tubes can have an isotropic shift up to 20 ppm larger than the atoms far from the ends. However, although not infinite, the SWCNTs present in experiment are quite long, so we do not expect this effect to contribute significantly to the NMR spectra.

(v) Other effects: Clearly every experimental sample of SWCNTs contains defects and magnetic impurities which will contribute to the broadening of the MAS peak. Furthermore, there may be interactions of the semiconducting nanotubes with the conduction electrons of metallic tubes contained in the bundle, etc.

We can see that effects (i)–(iii) can contribute around ~ 20 ppm to the width of the MAS peak. We therefore expect that the remaining ~ 10 – 30 ppm of the experimental width^{7,8,9} are due to (v). This means that by using better samples with a much lower concentration of magnetic impurities^{10,11} the resolution of ^{13}C NMR spectra can be improved by at most a factor of 2.

B. Anisotropic shifts

Also in Fig. 3 we show the principal values of the chemical shift tensor for the bundles. The first princi-

pal value, δ_{11}^{TMS} corresponds to the longitudinal (along the tube axis) direction, δ_{22}^{TMS} lies on the orthoradial direction, and δ_{33}^{TMS} is the radial component of the chemical shift tensor. As expected, the chemical shift is extremely anisotropic, with the longitudinal and orthoradial directions corresponding to the in-plane directions of a graphene sheet (or of a benzene molecule), and the radial component corresponding to the direction perpendicular to the sheet. As for the isotropic shift, the individual principal values are spread due to the interaction between the tubes in the bundle, but this time by as much as 10 ppm. Note that Ref. 8 found a value of 20 ppm for the broadening of the tensor due to the influence of the first neighbor tube (and quasi-independent on the electronic properties of this first neighbor). There is, therefore, a partial cancellation when we include all the six neighbors in the hexagonal lattice. Note that this 10 ppm spread is much larger than the 3 ppm spread of the isotropic line. It is also much larger than the difference between the two families of nanotubes we have studied.

In Fig. 4 we compare a simulation of the static spectrum of a (14,0) tube with experimental results. The theoretical spectrum shows a typical powder line-shape with principal values $\delta_{11}^{\text{TMS}} = 198$ ppm, $\delta_{22}^{\text{TMS}} = 188$ ppm, and $\delta_{33}^{\text{TMS}} = -11$ ppm ($\Delta\delta_{\text{anis}} = -204$ ppm and $\eta_{\text{C}} = 0.07$). The two experimental curves are quite different from each other, so care must be taken when comparing theoretical to experimental spectra. In general, we believe that our results are in quite good agreement with experiments. The main difference turns out to be the value for the asymmetry factor, which is considerably smaller in our calculations than in the experimental works.

V. DOUBLE-WALL TUBES

Recently, Simon *et al.* studied double-wall nanotubes using NMR²⁶. Their samples were produced through the high-temperature annealing of isotope enriched fullerenes encapsulated in single-wall tubes. In this way, they were able to measure directly the chemical shift of the inner tube. They found an isotropic shift of 111 ppm, which is significantly smaller than the isotropic shift of larger single wall tubes. The authors pointed out two possible reasons for this difference: (i) the stronger curvature of the inner tube, or (ii) diamagnetic shielding due to the outer tube. Note that in our calculations the chemical shift *increases* with decreasing radius (see Fig. 2), which rules out (i).

To study this problem, we performed *ab initio* calculations of the isolated double-wall tube (8,0)@(16,0). We obtained for the isotropic chemical shift of the atoms composing the inner tube a value of 111 ppm [to be compared with 132 ppm for the isolated (8,0) tube], implying a diamagnetic shift due to the outer tube of 21 ppm. On the other hand, the outer tube had an isotropic chemical shift of 126 ppm [to be compared to 124 ppm of the iso-

lated (16,0) tube]. Note that our *ab initio* result for the inner tube (111 ppm) coincides with the value measured in Ref. 26.

In order to understand our results, and to study the effect of diamagnetic shielding, we will resort to a simple classical model. Let us imagine that the outer nanotube has the form of a long hollow cylinder with axis parallel to \hat{z} . We will distinguish two cases, when the probing magnetic field $\mathbf{B}_0 \parallel \hat{z}$ and when $\mathbf{B}_0 \perp \hat{z}$. In the former case, the induced current \mathbf{j} on the surface of the cylinder can be written (in linear response) as $\mathbf{j} = \beta_{\parallel} B_0 \hat{\theta}$, where β_{\parallel} is a constant. The magnetization per unit length can then be calculated from (in cgs units)

$$\mathbf{M} = \frac{1}{2cL} \int d^3r \mathbf{r} \times \mathbf{j}(\mathbf{r}) = \frac{\beta_{\parallel} B_0 \pi D^2}{c} \hat{z}, \quad (4)$$

where c denotes the speed of light, L is the lattice parameter in the periodic direction, D is the diameter of the cylinder, and \hat{z} is the unit vector of direction z . The volume of integration is one unit cell. Remembering that $\mathbf{M} = \frac{\pi D}{N_A} n_C \chi_{\parallel} \mathbf{B}_0$, where χ_{\parallel} is the molar susceptibility parallel to the axis of the cylinder, N_A is the Avogadro number, and n_C is the density of carbon atoms per unit area of the nanotube ($n_C = 37.71 \text{ nm}^{-2}$), we can obtain the induced current

$$\beta_{\parallel} = c \frac{4n_C}{N_A D} \chi_{\parallel}. \quad (5)$$

On the other hand, it is a simple exercise of magnetostatics to calculate the magnetic field generated by \mathbf{B}_0 and by the induced current. The total magnetic field (\mathbf{B}_{in}) inside the cylinder (i.e., the field felt by the inner nanotube) is constant. Furthermore

$$\frac{B_{\text{in}} - B_0}{B_0} = 4\pi \frac{4n_C}{N_A D} \chi_{\parallel}. \quad (6)$$

Note that as $\chi_{V\parallel}$ is negative for our nanotubes, Eq. (6) gives rise to a *diamagnetic shift*. The same derivation can be done for an external field perpendicular to the tube axis. In this case, the current is, for a magnetization in the \hat{y} direction, $\mathbf{j} = \cos(\theta)\hat{z}$ on the sides of the cylinder, and $\mathbf{j} = \pm\beta_{\perp} B_0 \hat{x}$ on its bases. The total (external plus induced) field inside the tube is still constant, and it reads

$$\frac{B_{\text{in}} - B_0}{B_0} = 4\pi \frac{2n_C}{N_A D} \chi_{\perp}. \quad (7)$$

We can now calculate the diamagnetic shift in the inner tube due to the presence of the outer tube. As a typical example we chose the double-wall tube (8,0)@(16,0). Inserting its diameter (1.26 nm) and the calculated susceptibility ($\chi_{\parallel} = -9.60 \times 10^{-6} \text{ cgs/mol}$ and $\chi_{\perp} = -24.86 \times 10^{-6} \text{ cgs/mol}$) of the (16,0) tube in Eqs. (6) and (7) we obtain that the shift due to the shielding is $\delta_{33}^{\text{shield}} = -24 \text{ ppm}$ and $\delta_{11}^{\text{shield}} = \delta_{22}^{\text{shield}} = -31 \text{ ppm}$. This leads to an isotropic shift of $\delta_{\text{iso}}^{\text{shield}} = -29 \text{ ppm}$. From our calculations, the isotropic shift of the isolated (8,0) tube is 131 ppm, which leads to a total chemical shift for the inner tube of $\sim 102 \text{ ppm}$. This is a fairly good agreement with our *ab initio* results for such a crude model, and fully justifies its use in these systems.

VI. CONCLUSIONS

We performed calculations of the magnetic susceptibility and ^{13}C chemical shift for semiconducting zigzag carbon nanotubes, both isolated and in bundles. Our results are in very good agreement with experiment. For all nanotubes studied, the isotropic shift lies between 120 ppm and 135 ppm. This interval of 15 ppm is quite narrow, and is at the limit of the precision that NMR experiments have obtained for these systems. However, we expect that, with the advent of better samples, NMR will become a key tool to study and characterize carbon nanotubes.

Acknowledgments

The authors would like to thank S. Botti, C. Goze-Bac, and A. Rubio for fruitful discussions. MALM was supported by a Marie Curie Action of the European Commission, Contract No. MEIF-CT-2004-010384. Calculations were performed at the IDRIS supercomputing center (grant #051202).

-
- ¹ S. Iijima, *Nature (London)* **354**, 56 (1991).
 - ² M. Dresselhaus, G. Dresselhaus, and P. Avouris, *Carbon Nanotubes: Synthesis, Structure, Properties and Applications* (Springer-Verlag, Berlin Heidelberg, 2001).
 - ³ C. Kane, L. Balents, and M. P. A. Fisher, *Phys. Rev. Lett.* **79**, 5086 (1997).
 - ⁴ R. H. Baughman, A. A. Zakhidov, and W. A. de Heer, *Science* **297**, 787 (2002).
 - ⁵ V. Zólyomi and J. Kúrti, *Phys. Rev. B* **70**, 085403 (2004).
 - ⁶ D. M. Grant and R. K. Harris, *The Encyclopedia of NMR*

- (Wiley, London, 1996).
- ⁷ C. Goze-Bac, P. Bernier, S. Latil, V. Jourdain, A. Rubio, S. H. Jhang, S. W. Lee, Y. W. Park, M. Holzinger, and A. Hirsch, *Current Applied Physics* **1**, 149 (2001).
- ⁸ C. Goze-Bac, S. Latil, P. Lauginie, V. Jourdain, J. Conard, L. Duclaux, A. Rubio, and P. Bernier, *Carbon* **40**, 1825 (2002).
- ⁹ S. Hayashi, F. Hoshi, T. Ishikura, M. Yumura, and S. Ohshima, *Carbon* **41**, 3047 (2003).
- ¹⁰ K. Hata, D. N. Futaba, K. Mizuno, T. Namai, M. Yumura,

- and S. Iijima, *Science* **306**, 1362 (2004).
- ¹¹ S. Inoue, T. Nakajima, and Y. Kikuchi, *Chem. Phys. Lett.* **406**, 184 (2005).
 - ¹² A. Kitaygorodskiy, W. Wang, S.-Y. Xie, Y. Lin, K. A. Shiral Fernando, X. Wang, L. Qu, B. Chen, and Y.-P. Sun, *J. Am. Chem. Soc.* **127**, 7517 (2005).
 - ¹³ F. Mauri, B. G. Pfrommer, and S. G. Louie, *Phys. Rev. Lett.* **77**, 5300 (1996). F. Mauri, B. G. Pfrommer, and S. G. Louie, *Phys. Rev. B* **60**, 2941 (1999). C. J. Pickard and F. Mauri, *Phys. Rev. B* **63**, 245101 (2001).
 - ¹⁴ “PARAllel Total Energy Code”, <http://www.nersc.gov/projects/paratec/>.
 - ¹⁵ C. G. van de Walle and P. E. Blöchl, *Phys. Rev. B* **47**, 4244 (1993).
 - ¹⁶ J. L. Martins and N. Troullier, *Phys. Rev. B* **46**, 1766 (1992).
 - ¹⁷ E. Zurek and J. Autschbach, *J. Am. Chem. Soc.* **126**, 13079 (2004).
 - ¹⁸ A. K. Jameson and C. J. Jameson, *Chem. Phys. Lett.* **134**, 461 (1987).
 - ¹⁹ H. Ajiki and T. J. Ando, *Phys. Soc. Japan* **64**, 4382 (1995).
 - ²⁰ J. P. Lu, *Phys. Rev. Lett.* **74**, 1123 (1995).
 - ²¹ S. Zaric, G. N. Ostojic, J. Kono, J. Shaver, V. C. Moore, R. H. Hauge, R. E. Smalley, and X. Wei, *Nanolett.* **4**, 2219 (2004).
 - ²² X.-P. Tang, A. Kleinhammes, H. Shimoda, L. Fleming, K. Y. Bennoune, S. Sinha, C. Bower, O. Zhou, and Y. Wu, *Science* **288**, 492 (2000).
 - ²³ S. Latil, L. Henrard, C. Goze-Bac, P. Bernier, and A. Rubio, *Phys. Rev. Lett.* **86**, 3160 (2001).
 - ²⁴ J. A. Pople, *J. Chem. Phys.* **37**, 53 (1962).
 - ²⁵ P. Lauginie, H. Estrade-Szwarckopf, B. Rousseau, and J. Conard, *CR. Acad. Sci. Paris* **307II**, 1693 (1998).
 - ²⁶ F. Simon, C. Kramberger, R. Pfeiffer, H. Kuzmany, V. Zólyomi, J. Kürti, P. M. Singer, and H. Alloul, *Phys. Rev. Lett.* **95**, 017401 (2005).
 - ²⁷ The isotropic chemical shift is defined as the trace of the chemical shift tensor divided by 3, i.e., $\delta_{\text{iso}} = (\delta_{11} + \delta_{22} + \delta_{33})/3$. The individual components are usually assigned such that $|\delta_{33} - \delta_{\text{iso}}| \geq |\delta_{11} - \delta_{\text{iso}}| \geq |\delta_{22} - \delta_{\text{iso}}|$. The magnitude of the chemical shift anisotropy is $\Delta\delta_{\text{anis}} = (3/2)(\delta_{33} - \delta_{\text{iso}})$ and the asymmetry factor $\eta_C = (\delta_{22} - \delta_{11})/(\delta_{33} - \delta_{\text{iso}})$.